212 *Journal of Electrical Engineering & Technology Vol. 7, No. 2, pp. 212~220, 2012*
http://dx.doi.org/10.5370/JEET.2012.7.2.212

Optimization Shape of Variable-Capacitance Micromotor Using Seeker Optimization Algorithm

Abbas Ketabi† and Mohammad Javad Navardi*

Abstract – In the current paper, the optimization shape of a polysilicon variable-capacitance micromotor (VCM) was determined using the seeker optimization algorithm (SOA). The optimum goal of the algorithm was to find the maximum torque value and minimum ripple torque by varying the geometrical parameters. The optimization process was performed using a combination of SOA and the finite-element method (FEM). The fitness value was calculated via FEM analysis using COMSOL3.4, and SOA was realized by MATLAB7.4. The proposed method was applied to a VCM with eight and six poles at the stator and rotor, respectively. For comparison, this optimization was also performed using the genetic algorithm. The results show that the optimized micromotor using SOA had a higher torque value and lower torque ripple, indicating the validity of this methodology for VCM design.

Keywords: Variable-capacitance micromotor (VCM), Finite-element method (FEM), Seeker optimization algorithm (SOA), Micromotor optimization, MEMS

1. Introduction

The variable-capacitance micromotor (VCM) is an important MEMS actuator [1] for several applications, such as medical implants, optical systems, microrobotics, and aeronautics and space applications [2]. The electrostatic field of a VCM is analyzed using FEM because of the difficulties in calculating the electric field at the edges [3].

However, less attention has been given to the optimization of the VCM design geometry. An exhaust algorithm based on 5% steps of each design parameter has been used in VCM optimization [4], for which every combination of different variables was analyzed using FEM. However, the results were inaccurate, and the calculation time was reported to be long [5].

The current paper proposes a new method for VCM optimization based on the seeker optimization algorithm (SOA). SOA is a relatively new intelligent algorithm that may be used to find optimal (or near-optimal) solutions to numerical and qualitative problems. This algorithm simulates the human searching behavior originally proposed in [6], which regards the optimization process as a search for the optimal solution using a seeker population. Each individual or candidate solution is a vector that contains as many parameters as those of the problem dimensions. This technique is a robust optimization tool [7]. Thus, its application in VCM optimization is proposed in the current paper. A combination of the improved SOA and FEM analysis is performed to get the optimization shape of the micromotor. The fitness value is calculated using COMSOL3.4, and the genetic algorithm is realized using MATLAB7.4.

The current paper is organized as follows. Section 2 describes the torque calculation and excitation sequence of the VCM. Section 3 proposes a cost function and its control parameters to define the optimization problem. A detailed description of SOA and its associated parameter tuning are presented in Section 4. The implementation of SOA in geometrical optimization and the comparison of its performance with that of GA, as well as the comparison between the optimized and typical micromotors, are discussed in Section 5. Finally, the conclusions are drawn in Section 6.

2. VCM

The cross section of the micromotor investigated in the current study is shown in Fig. 1. The rotor and stator are made from polysilicon films, and the medium between them is air. The modeled VCM has eight stator electrodes grouped in four phases and six rotor poles, and it is excited with 100 V. The stator and rotor have outer radii (R_{os} and R_{or}) of 100 and 50 μm, respectively. The gap between an aligned rotor and a stator pole is 1.5 μm. The angular width of both stator and rotor electrodes (φ_s and φ_r) is 18°, and the slot radius of the micromotor R_{ir} is 30 μm. The axial thickness of the rotor and stator is 2.2 μm [1].

2.1 Mathematical model of VCM

An electrostatic motor works based on the action of the

† Corresponding Author: Department of Electrical Engineering, University of Kashan, Kashan, Iran (aketabi@kashanu.ac.ir).
* Department of Electrical Engineering, I.A.U. Kashan Branch, Kashan, Iran (navardi@iaukashan.ac.ir).
Received: May 31, 2010; Accepted: October 29, 2011

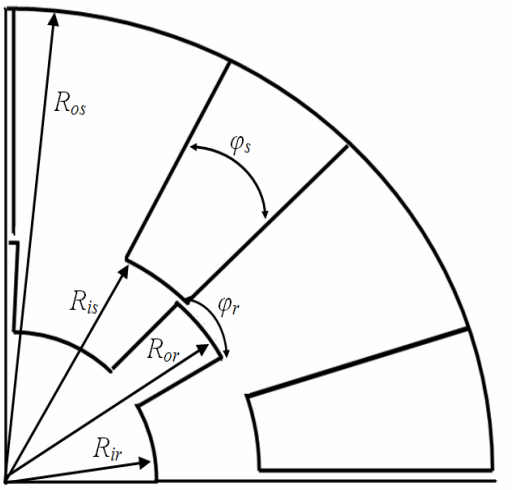

Fig. 1. Micromotor configuration and geometrical parameters

columbic forces in the gap between the stator and rotor [8]. When voltage is applied between the rotor and stator electrodes, the resulting electrostatic force aligns the electrodes. This type of micromotor demonstrates the concept of storing electrical energy within a variable stator–rotor capacitance [9]. Modeling the operation of the micromotor involves solving the electrostatic component of Maxwell's equation for force and, therefore, torque. Using the finite-element method (FEM), the second-order partial differential equation is solved for the electric scalar potential V surrounding the stator and rotor poles of the micromotor [10]

$$-\varepsilon \nabla^2 V = \rho \tag{1}$$

where ε is the electrical permittivity of the surrounding region and ρ is the charge density distribution on the rotor and stator. The electric field intensity E and electric flux density D can then be calculated from the following [10]:

$$E = -\nabla V \tag{2}$$

$$D = \varepsilon . E \, . \tag{3}$$

Various methods can be used to compute the electrostatic forces in an electromechanical energy conversion device. The most commonly methods are [11] the following:

(1) stress tensor method

(2) co-energy method.

The electrostatic force densities at every point on a closed contour located in the air gap of the machine can be calculated using the Maxwell stress tensor method. However, the torque computed by this method does not consider the torque ripples [12].

For the co-energy method, the electrostatic energy must first be calculated to obtain the electrostatic torque as a function of the rotor position. This energy is proportional to the capacitance between the stator and rotor [13]. The stored energy in the electric field within the micromotor is obtained using the following:

$$W' = \frac{1}{2} C(\theta) . V^2 \tag{4}$$

where C is the capacitance between the stator and rotor with respect to the angular rotor position θ and V is the applied potential at the electrodes. The tangential component of the electrostatic force is calculated by differentiating the total co-energy with respect to the position of the rotor for single-phase excitation as follows [13]:

$$T(\theta) = \frac{\partial W'}{\partial \theta} = \frac{1}{2} . \frac{\partial C(\theta)}{\partial \theta} . V^2 \, . \tag{5}$$

This method provides a relatively straightforward solution. In the current study, the 2-D FEM is used to analyze the electrostatic field in the micromotor. Considering that the electrostatic micromotor is an electrically linear system [14], the driving torque is calculated per meter of axial thickness and then multiplied by the actual axial thickness. The voltage distribution at the rotor position of 15° is illustrated in Fig. 2. At all points, the electric fields are perpendicular to the equipotential lines. For the energy calculation, one pair of stator electrodes is supplied with a constant voltage, whereas the other stator electrodes, as well as the rotor, are grounded. The angular distance that the rotor must travel to move from the alignment with one stator phase to the next is 60°. Once the electrodes are aligned, the excitation to that pair of stator electrodes is switched off, and the subsequent pair is excited. At each rotor position, the stored energy in the electric field can be evaluated as a function of the rotor position. The rotor moves through an angle of 1° between

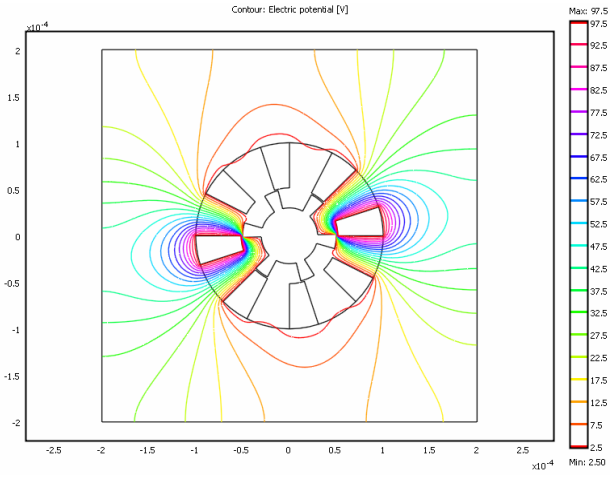

Fig. 2. Micromotor geometry showing the equipotential lines at $\theta = 15°$

the active stator electrodes. Hence, within each rotor pole pitch, 60 positions are obtained. In the current work, a continuous curve is fitted to energy–angle points using the spline interpolation technique, which is considered to be an effective tool for such data fitting [15].

The function of energy versus angle is then obtained, from which the torque can be calculated as the partial derivative of energy versus the angular displacement. Fig. 3 demonstrates the torque profile versus the rotor position for different phase excitations. Therefore, the torque obtained from the co-energy method is a function of the rotor position and has average and ripple components. As aforementioned, in a 2-D FEM, the driving torque is calculated per meter of axial thickness. Considering that the electrostatic micromotor is a linear system, the torque has to be multiplied by the actual axial thickness.

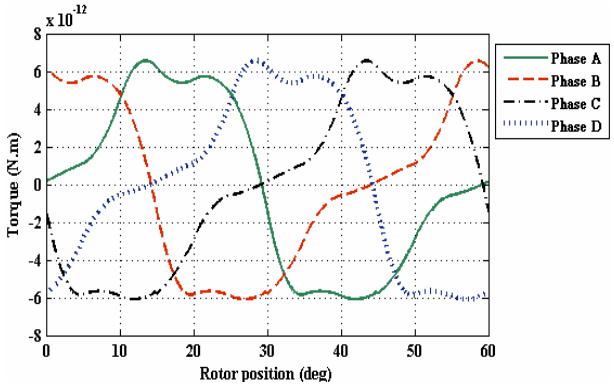

Fig. 3. Torque–angle curves during one electric period for the excitation schemes from *phase A* to *D*

2.2 Excitation sequence

A detailed knowledge of the force distribution in a micromechanical system such as a micromotor is very important in the analysis of such devices [16]. The forces exerted on the rotor act in three major orientations: axial, radial, and rotational. High tangential forces are necessary in torque maximization. However, axial and radial components should be minimized [16]. Therefore, the excitation should be applied symmetrically. Fig. 4 illustrates the symmetrically excited sequence (excitation schemes from *phases A* to *D*) for the micromotor used in the current work. The black electrodes in the figure are excited with 100 V, whereas the rotor and other stator electrodes are grounded as stated previously.

The torque–angle curves are obtained for each excitation scheme using this excitation sequence. A smooth generated torque is achieved at the crossover by switching from one excitation scheme to another (Fig. 3). Fig. 5 shows the generated torque during one electric period for the optimal excitation sequence. As shown, the torque ripple has been minimized in the resulting sequence.

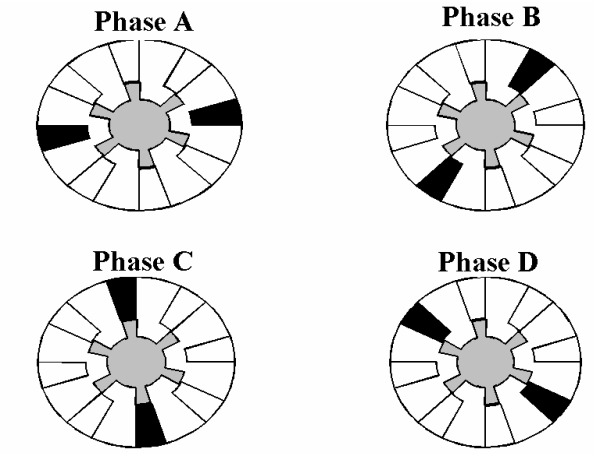

Fig. 4. Symmetric excitations of a micromotor with eight stator electrodes

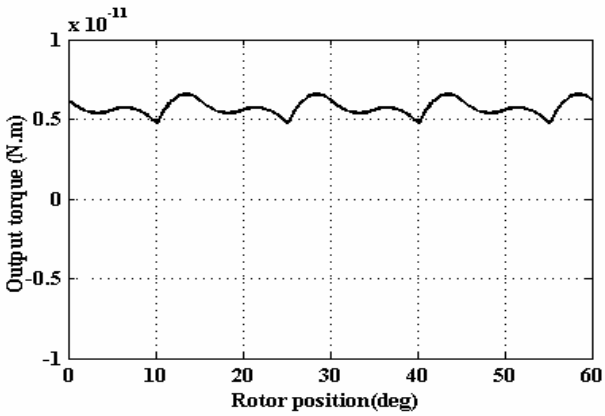

Fig. 5. Output torque distribution

3. Fitness Function and Control Geometric Variables of the Micromotor

The choice of an appropriate objective function is crucial for any procedure regardless of the optimization method used. The current paper aims to determine the optimum geometrical structure for the VCM with the maximum torque value and minimum ripple factor [5]. Therefore, the proposed objective function must satisfy these conditions. In the current work, we have investigated two terms for the objective function. The first (6) corresponds to the maximum torque component, for which the effective value of the torque in one electrical period is considered

$$T_{rms} = \sqrt{\frac{1}{\tau}\int_0^{\tau} T(\theta)^2 .d\theta} \ . \tag{6}$$

Here, $T(\theta)$ is the electrostatic torque at rotor position θ and τ is the electrical period that is equal to 60°.

The second term corresponds to the minimum torque ripple factor *R.F* defined as follows:

$$R.F = \frac{T_{ac}}{T_{ave}} \tag{7}$$

where

$$T_{ave} = \frac{1}{\tau}\int_0^{\tau} T(\theta).d\theta \tag{8}$$

$$T_{ac} = \sqrt{{T_{rms}}^2 - {T_{ave}}^2}\ . \tag{9}$$

T_{ave}, T_{ac}, and $R.F$ are the average torque, the AC component of the torque curve, and the ripple factor of the output torque, respectively. In the FEM analysis, the torque is computed from the obtained nonlinear solution of the voltage using (1) to (5). The closed contour in the middle of the air gap is used as the path of integration. The objective function which will satisfy both conditions of maximum torque and minimum ripple is a weighted sum of both objective functions $f(x)$ defined as

$$f(x) = m.\frac{T_{rms0}}{T_{rms}} + \frac{R.F}{R.F_0} \tag{10}$$

where T_{rms0} and $R.F_0$ are the effective torque and the ripple factor for a typical micromotor, respectively. m is the weight factor for the torque term and is assumed to be 2. With the above presentation of $f(x)$, the optimization procedure takes place by simply minimizing $f(x)$.

The dependency of the objective function $f(x)$ on its parameters x is unknown, whereas the value of the objective function can be computed using FEM for each generated set of parameters x. The optimization therefore aims to find the set of parameters x for which the value of the objective function is minimum.

For the optimization parameters, several geometrical parameters could be used as variables. Some of these are independent variables, whereas others are dependent on other geometric parameters. Letting all parameters vary independently would make the optimization procedure too complex. A good convergence can be achieved if the optimization function parameters are independent [17]. The independent design parameters considered in the current work are the stator and rotor pole widths and the rotor inner radius (Fig. 1). However, some physical constraints need to be considered. In a real VCM, the rotor cannot overlap the stator, and the stator poles cannot overlap each other. Table 1 shows the boundary constraints for these design parameters to avoid the violation of physical laws.

Table 1. Control geometric variables and their limits.

Symbol	Control parameters	Limits of control parameters
φ_s	Stator pole width	$15° < x_1 < 44°$
φ_r	Rotor pole width	$15° < x_2 < 59°$
R_{ir}	Rotor inner radius	$20\ \mu m < x_3 < 50\ \mu m$

4. SOA

Evolutionary algorithms such as SOA are a good choice for the optimization of the electromagnetic device parameters [18]. In SOA, the next position of each seeker is obtained from its current position based on its historical and social experience. This method searches the optimal solutions around the current positions until it converges to the optimum. Then, it does not easily get lost and is able to locate the region where the global optimum exists, subsequently converging to the optimum.

In SOA, the position of each seeker, which is updated on each dimension, is given by the following:

$$x_{ij}(t+1) = x_{ij}(t) + \alpha_{ij(t)} d_{ij}(t) \tag{11}$$

where $\alpha_{ij}(t)$ and $d_{ij}(t)$ are the search direction and step length of each seeker i, respectively, on each dimension j for time step t, where $\alpha_{ij}(t) \geq 0$ and $d_{ij}(t) \in \{-1,0,1\}$. In (11), if $d_{ij}(t) = 1$, the ith seeker goes to the positive orientation of the coordinate axis on dimension j. If $d_{ij}(t) = -1$, the seeker goes to the negative orientation, and if $d_{ij}(t) = 0$, the seeker stays at the current position. The convergence of the subpopulations to local minima is avoided by combining the position of the worst k-1 seeker of each subpopulation with the best in each of the other k-1 subpopulations using the following binomial crossover operator:

$$x_{k_n j,worst} = \begin{cases} x_{lj,best} & if\ \ R_j \leq 0.5 \\ x_{k_n j,worst} & else \end{cases} \tag{12}$$

where R_j is a uniformly random real number within [0, 1] and $x_{knj,worst}$ denotes the jth dimension of the nth worst position in the lth subpopulation.

In SOA, the search direction of each seeker is determined based on several empirical gradients (EGs) by comparing the current or epochal positions of itself or its neighbors. The corresponding EG can be involved

$$\vec{d}_{i,ego}(t) = sign(\vec{p}_{i,best}(t) - \vec{x}_i(t)) \tag{13}$$

$$\vec{d}_{i,alt_1}(t) = sign(\vec{g}_{i,best}(t) - \vec{x}_i(t)) \tag{14}$$

$$\vec{d}_{i,alt_2}(t) = sign(\vec{l}_{i,best}(t) - \vec{x}_i(t)) \tag{15}$$

where $d_{i,ego}(t)$ is the egotistic direction and $d_{i,alt1}(t)$ and $d_{i,alt2}(t)$ are the altruistic directions of seeker i. $p_{i,best}(t)$, $g_{i,best}(t)$, and $l_{i,best}(t)$ are the personal historical best position, the historical best position of the neighbors, and the current best position of the neighbors, respectively. $sign(\cdot)$ is a signum function on each dimension of the input vector, and $x_i(t) = [x_{i1}, x_{i2}, \ldots, x_{iD}]$ is the position of the ith seeker at time step t. In this algorithm, each seeker i can earn an EG by appraising his latest positions

$$x_{ij}(t+1) = x_{ij}(t) + \alpha_{ij(t)} d_{ij}(t) \tag{16}$$

where t_1 and $t_2 \in \{t, t\text{-}1, t\text{-}2\}$ and $x_i(t_1)$ is better than $x_i(t_2)$. Every dimension j of the search direction of the ith seeker, denoted as $d_i(t)$, is selected using the following proportional selection rule:

$$\begin{cases} 0 & if\ r_j \le p_j^{(0)} \\ +1 & if\ p_j^{(0)} < r_j \le p_j^{(0)} + p_j^{(+1)} \\ -1 & if\ p_j^{(0)} + p_j^{(+1)} < r_j \le 1 \end{cases} \tag{17}$$

where r_j is a uniform random number in [0,1] and $p_j^{(m)}$ ($m \in \{0,1,-1\}$) is the percentage of the number of m from the set $\{d_{ij,ego}(t), d_{ij,alt1}(t), d_{ij,alt2}(t), d_{ij,pro}(t)\}$ on each dimension j of all the four empirical directions, that is

$$p_j^{m} = \frac{the\ number\ of\ m}{4}.$$

In SOA, a fuzzy system is used to simulate the human searching behavior. In this algorithm, the fitness values of all the seekers are sorted in descending order and converted into sequence numbers from 1 to s as the fuzzy reasoning inputs. The current work prepares a fuzzy system to a wide range of optimization problems to earn the first step length

$$\mu_i = \mu_{\max} - \frac{s - I_i}{s-1}(\mu_{\max} - \mu_{\min}) \tag{18}$$

where I_i is the sequence number of $x_i(t)$ after sorting the fitness values and μ_{max} is the maximum membership degree value equal to or slightly less than 1. Then, the Bell membership function $\mu(x) = e^{-x^2/2\delta^2}$ is used in the action part of the fuzzy reasoning. δ is the parameter of the Bell membership function, which is determined by the following:

$$\vec{\delta} = \omega.abs(\vec{x}_{best} - \vec{x}_{rand}) \tag{19}$$

where $abs(\cdot)$ produces an output vector. ω is used to decrease the step length as the time step increases. Thus, the search accuracy is gradually improved. x_{best} and x_{rand} are the best seeker and a randomly selected seeker from the same subpopulation to which the ith seeker belongs, respectively [6-7, 19]. The step length is determined as follows:

$$\alpha_{ij} = \delta_j \sqrt{-\ln(\mu_{ij})} \tag{20}$$

where

$$\mu_{ij} = RAND(\mu_i, 1) \tag{21}$$

The flowchart of the VCM optimization based on SOA is shown in Fig. 6. The population is randomly categorized into $K = 3$ subpopulations to search over several different domains of the search domain. The upper and lower bounds of the state variables are required to initialize the seeker's position. The upper and lower bounds for the SOA used in this problem are listed in Table 1. The other parameters of SOA are $\omega=0.9$, $\mu_{min}=0.0111$, and $\mu_{max}=0.97$.

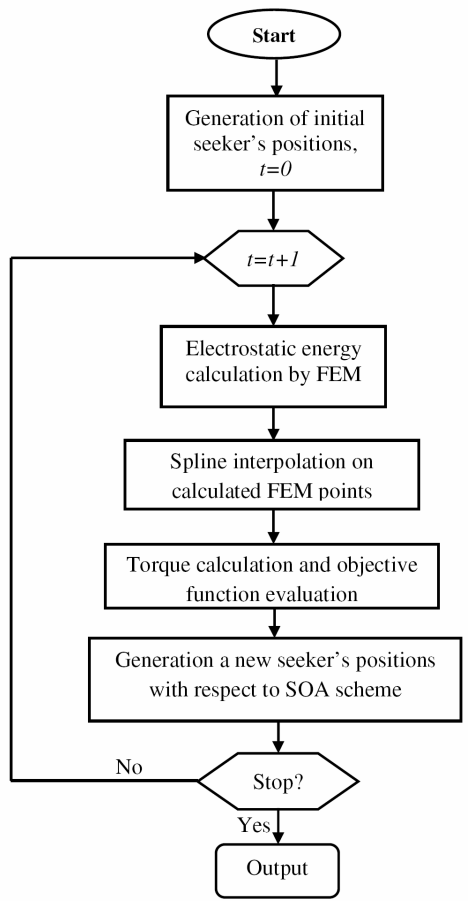

Fig. 6. Illustration of the micromotor optimization

4. Simulation Results

In the current work, three optimization processes were performed: the maximization of the torque, minimization of the ripple factor, and simultaneous optimization of both. The characteristics of the optimized and typical micromotors are compared using the following parameters:

$$\%\Delta T_{rms} = \frac{T_{rms} - T_{rms0}}{T_{rms0}} \times 100 \tag{22}$$

$$\%\Delta R.F = \frac{R.F - R.F_0}{R.F_0} \times 100 \tag{23}$$

where $\%\Delta T_{rms}$ and $\%\Delta R.F$ are the percentage changes of the torque and ripple factor, respectively. The parameters of

the typical micromotor shown in Fig. 1 are given in Table 2.

The performance of the proposed SOA was investigated by performing the VCM optimization using GA with a large population size of 80 and rather large generation number of 100, with a crossover probability of 0.5 and mutation probability of 0.1.

Table 2. Parameters of a typical VCM.

Parameters	Nonoptimized VCM
Stator pole width φ_s	18°
Rotor pole width φ_r	18°
Rotor inner radius R_{ir}	30 μm
Ripple factor $R.F_0$	0.00393
Torque T_{rms}	5.6658 pN·m

As shown in the flowchart in Fig. 6, in optimizing a VCM with SOA (or GA) and FEM, both must be adjusted for them to function in a coordinated manner. This condition indicates that, in evaluating the objective function of a design parameter set (individual), the FEM package must be able to accept the parameters generated by SOA (or GA) for it to perform the FEM computation automatically. Moreover, it must be able to return the value of the objective function to the optimization algorithm. All algorithms are run in MATLAB7.4.0 where COMSOL 3.4 is used for the FEM analysis. This computation is performed using a PC with Pentium 4 quad-core CPU (2.83 GHz) and 4 GB RAM.

4.1 Maximization of the torque value

Considering (6), the objective function for this optimization process is

$$f(x) = \frac{T_{rms0}}{T_{rms}}. \tag{24}$$

As shown in the optimization results in Table 3, SOA offers both shorter run-time and higher torque values than those of GA.

Fig. 7 demonstrates the convergence curve of the objective function against the iteration number for the SOA. It reached a minimum of about 0.9394 after 20 iterations in almost 30 h of run time. Fig. 8 shows the graphs of torque versus angle for the typical and SOA-optimized micromotors. Despite the increase in ripple factor, the optimization increased the torque value of the VCM by more than 6.5%.

4.2 Minimization of the torque ripple

Considering (7), the objective function for the ripple factor minimization can be defined by

$$f(x) = \frac{T_{rms0}}{T_{rms}} \tag{25}$$

Table 3. VCM parameters for the torque optimization.

Parameter	SOA	GA
Stator pole width φ_s	30.3910°	30.1449°
Rotor pole width φ_r	16.5357°	16.4162°
Rotor inner radius R_{ir}	20.4267 μm	20.738 μm
Ripple factor $R.F_0$	0.1317	0.1360
Torque T_{rms}	6.0357 pN·m	6.033 pN·m
Objective function $f(x)$	0.9394	0.9399
Population size Np	30	80
Number of iterations G	50	100
Run time	30 h	160 h

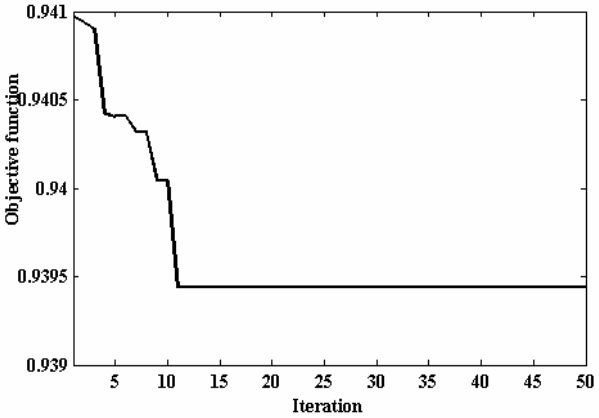

Fig. 7. Convergence curves of SOA for the torque optimization

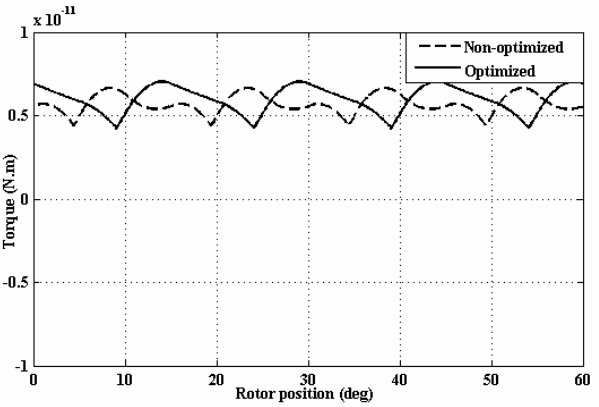

Fig. 8. Torque profile after torque optimization compared with that of the nonoptimized torque

The geometric parameters for the SOA- and GA-optimized micromotors are listed in Table 4.

SOA yields improved results in terms of both the optimization elapsed time (due to the smaller population size and lesser number of iterations) and the ripple factor.

The convergence process for the SOA is illustrated in Fig. 9. The torque–angle curves of the typical and optimized VCMs are compared in Fig. 10, which indicates a substantial decrease in the ripple factor (almost 95%). The value of the torque was also decreased.

Table 4. VCM parameters for the ripple minimization.

Parameter	SOA	GA
Stator pole width φ_s	21.6849°	25.7853°
Rotor pole width φ_r	23.2280°	28.4421°
Rotor inner radius R_{ir}	45.9868 μm	47.897 μm
Ripple factor $R.F_0$	0.00015	0.0019
Torque T_{rms}	4.7219 pN·m	3.869 pN·m
Objective function $f(x)$	0.0040	0.0480
Population size Np	30	80
Number of iterations G	100	100
Run time	60 h	160 h

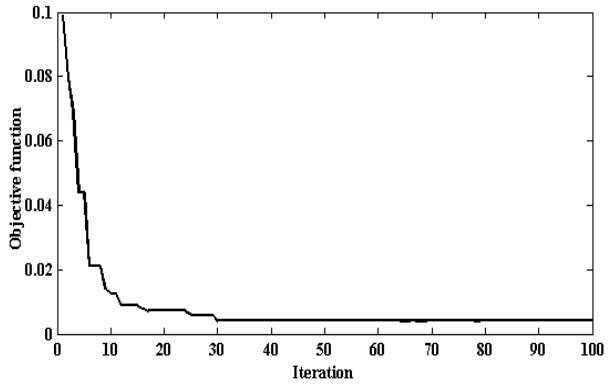

Fig. 9. Convergence curves of SOA for the ripple optimization

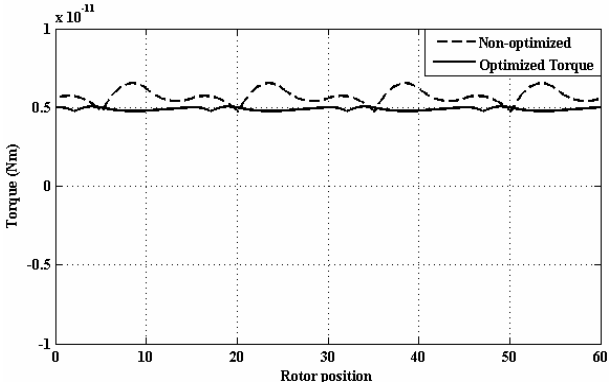

Fig. 10. Torque profile after ripple optimization compared with that of the nonoptimized torque

4.3 Simultaneous maximization of the torque and minimization of the ripple

The objective function for the simultaneous torque maximization and ripple minimization is defined in (10). The geometric parameters for this aim using SOA and GA are shown in Table 5. Again, the optimization results in Table 5 indicate that SOA offers both shorter run-time and higher torque values than those of GA.

Fig. 11 shows the convergence process using SOA after 40 iterations. The corresponding torque–angle curve indicating a 2.5% increase in the torque value and 82% decrease in the ripple factor is shown in Fig. 12.

Table 5. VCM parameters for the torque and ripple optimization.

Parameter	SOA	GA
Stator pole width φ_s	27.9317°	28.369°
Rotor pole width φ_r	23.9762°	22.864°
Rotor inner radius R_{ir}	23.1135 μm	25.504 μm
Ripple factor $R.F_0$	0.0061	0.0075
Torque T_{rms}	5.801 pN·m	5.863 pN·m
Objective function $f(x)$	2.1087	2.1259
Population size Np	30	80
Number of iterations G	50	100
Run time	30 h	160 h

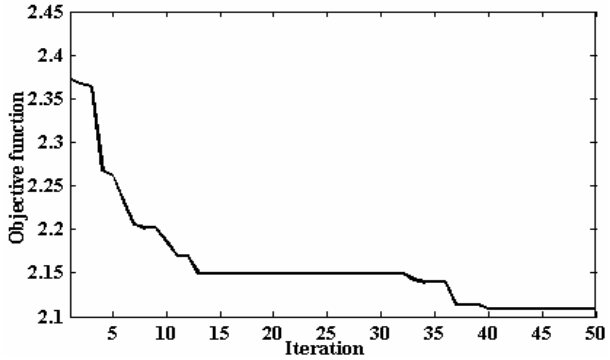

Fig. 11. Convergence curves of SOA for the simultaneous torque and ripple optimization

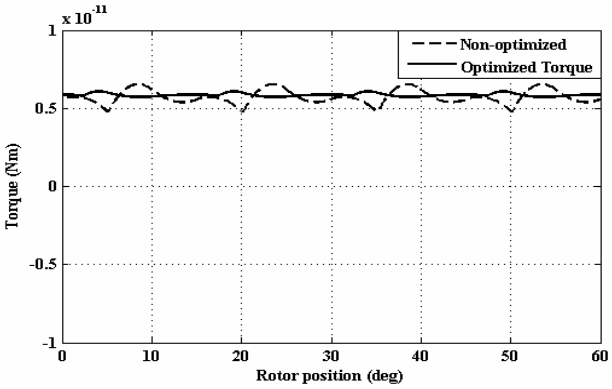

Fig. 12. Torque profile after the torque and ripple optimization compared with that of the nonoptimized torque.

5. Conclusion

In the current paper, following the description of the operation principles of a VCM, a combined application of SOA (or GA) with FEM analysis for the torque calculations was presented. Using spline interpolation, a continuous curve was fitted to the energy–angle points, from which the torque was then calculated via differentiation. After the appropriate independent geometrical parameters for the micromotor optimization were selected, a suitable objective function was presented. Using SOA, which is a powerful evolutionary computation

technique, a typical VCM is optimized in conjunction with FEM. All algorithms were implemented in the MATLAB environment. The proposed method was verified using a VCM with eight and six stator and rotor poles, respectively.

The comparison of the results with the values of a typical micromotor shows the enhanced torque value and decreased torque ripple, indicating improved efficiency in the VCM performance. Compared with GA, SOA reaches the optimal solutions faster with lesser objective functions. Hence, this approach could well be applied in the optimization of the performances of other MEMS devices.

References

[1] Stephen, F.B., Mehran, M., Lee, S.T., Jeffrey, H.L., and Stephen, D.S, "Electric micromotor dynamics," *IEEE Trans. Electron Devices*, vol. 39, pp. 566-575, Mar. 1992.

[2] T. C. Neugebauer, D. J. Perreault, J. H. Lang, C. Livermore, "A Six-Phase Multilevel Inverter for MEMS Electrostatic Induction Micro-motors," *IEEE Trans. Circuits and Systems II: Express Briefs,* vol. 51, pp. 49-56, Feb. 2004.

[3] Zhang, W.; Meng, G.; Li, H., "Electrostatic Micromotor and its Reliability," *Microelectronics Reliability*, vol. 45, pp. 1230-1242, July-August. 2005.

[4] V.Bahjat and A.Vahedi, "Minimizing the torque ripple of variable capacitance electrostatic micromotors," *Journal of Electrostatics*, vol. 64, pp. 361-367, June. 2006.

[5] Johansson, T.B.; Van Dessel, M.; Belmans, R.; Geysen. W, "Technique for finding the optimum geometry of electrostatic micromotors," *IEEE Trans. Industry Applications*, vol. 30, pp. 912-919, Jul/Aug 1994.

[6] Chaohua Dai, Weirong Chen and Yunfang Zhu, "Seeker Optimization Algorithm". *IEEE Int. Conf. on Computational Intelligence and Security,* 2006, Vol. 1, pp. 229–248.

[7] Chaohua Dai, Weirong Chen, Yunfang Zhu and Xuexia Zhang, "Seeker Optimization Algorithm for Optimal Reactive Power Dispatch". *IEEE Transactions on Power Systems*, vol. 24, pp. 1218 – 1231, 2009.

[8] W.K.S. Pao, W.S.H. Wong and A. M. K. Lai, "An explicit drive algorithm for aiding the design of firing sequence in side-drive micromotor," *Communications in Numerical Methods in Engineering*, vol. 24, pp. 2131-2136, Dec. 2008.

[9] Sujay S. Irudayaraj and Ali Emadi, "Micromachines: Principles of Operation, Dynamics, and Control," in *IEEE Int. Conf. Electric Machines and Drives,* 2005, pp. 1108–1115.

[10] Delfino, F.; Rossi, M, "A new FEM approach for field and torque simulation of electrostatic microactuators," *IEEE J. Microelectromechanical Systems*, vol. 11, pp. 362–371, Aug. 2002.

[11] Long Sheng Fan, Yu-Chung Tai, Richard S. Muller, "IC-Processed Electrostatic Micro-motors," in *IEEE Int. Conf. Electron Devices Meeting,* 1988, pp. 666–669.

[12] A. Jindal, M.Krishnamurthy, B. Fahimi, "Micromachines: Principles of Operation, Dynamics, and Control," in *IEEE Int. Conf. Power Electronics, Electrical Drives, Automation,* 2005, pp. 358–365.

[13] S.Wiak, P. Di Barba and A. Savini, "3-D Computer Aided Analysis of the "Berely" Electrostatic Micromotor," *IEEE Trans. Magnetics*, vol. 31, pp. 2108–2111, May. 1995.

[14] Behjat. V,.Vahedi. A, "Analysis and Optimization of MEMS Electrostatic Microactuator," in *IEEE Int. Conf. Perspective Technologies and Methods in MEMS Design,* 2007, pp. 20–25.

[15] Larry Schumaker, *Spline Functions: Basic Theory*, Cambridge University Press, 2007, ch.1.

[16] Milne, N.G.; Yang, S.J.E.; Sangster, A.J.; Ziad, H.; Spirkovitch, S, "Determination of the forces present in an electrostatic micromotor," in *IEEE Int. Conf. Electrical Machines and Drives*, 1993, pp. 9–14.

[17] J. U. Duncombe, "Infrared navigation—Part I: An assessment of feasibility (Periodical style)," *IEEE Trans. Electron Devices*, vol. ED-11, pp. 34–39, Jan. 1959.

[18] Stumberger, G. Dolinar, D. Palmer, U. Hameyer, K, "Optimization of radial active magnetic bearings using the finite element technique and the differential evolution algorithm," *IEEE Trans. Magnetics*, vol.36, pp. 1009–1013, Jul. 2000.

[19] Michalewicz. Z, "Seeker Optimization Algorithm for Digital IIR Filter Design", *IEEE Transactions on Industrial Electronics*, vol. 57, pp. 1710 - 1718, 2010.

Abbas Ketabi He received the B.Sc. and M.Sc. degrees in electrical engineering from the Department of Electrical Engineering, Sharif University of Technology, Tehran, Iran, in 1994 and 1996, respectively, and the Ph.D. degree in electrical engineering jointly from Sharif University of Technology and the Institut National Polytechnique de Grenoble, Grenoble, France, in 2001. Since then, he has been with the Department of Electrical Engineering, University of Kashan, Kashan, Iran, where he is currently an Associate Professor. He has published more than 50 technical papers and three books. He is the Manager and an Editor of *Energy Management*. His research interests include the optimization shape of electric machines and evolutionary computation. Dr. Ketabi was the recipient of the University of Kashan Award for Distinguished Teaching and Research.

Mohammad Javad Navardi He was born in Kashan, Iran, in 1985. He received the B.Sc. and M.Sc. degrees in electrical engineering from the Department of Electrical Engineering, University of Kashan, Kashan, in 2007 and 2009, respectively. He is currently with the Department of Electrical Engineering, Islamic Azad University of Kashan. His research interests include microelectromechanical systems modeling and simulation, finite-element method, optimization shape of electric machines, and soft computing methods.